Published by IOP Publishing for Sissa Medialab

Received: *January 17, 2020*
Accepted: *March 11, 2020*
Published: *April 14, 2020*

Feasibility of underwater radiation detector using a silicon photomultiplier (SiPM)

Jeong Ho Kim[a,1] **and Koan Sik Joo**[b]

[a] *Institute of Radiation Medicine, Seoul National University Medical Research Center, Seoul, Korea*
[b] *Department of Physics, University of Myongji, Yongin, Korea*

E-mail: jeongho5248@gmail.com

Abstract: In this paper, the development of an underwater radiation detector is presented using a silicon photomultiplier (SiPM), CsI(Tl) scintillator, and light guide. The detector characteristics were evaluated. The detector has good energy resolution characteristics in which the gamma-ray emission energy 122 keV of ^{57}Co had an energy resolution of 18.12%, 356 keV of the ^{133}Ba spectrum had 10.91%, 662 keV of the ^{137}Cs spectrum had 8.84%, and 1332 keV of the of the ^{60}Co spectrum had 4.55%. Further, in the case of mixed sources, the gamma radiation peaks were readily distinguishable, and the R-squared value in the gamma-ray energy of 122–1332 keV for energy linearity was calculated to be 0.99937, demonstrating an exceptional energy linearity. In addition, radiative contaminated water was prepared as a liquid radiation source and characterized. The measurement results showed 0.61 ±0.0046 cps in the background and 0.74 ±0.0070 cps at the minimum concentration of 38.71 Bq/L. The R-squared value for concentrations in the range of 38.71–4955 Bq/L, which indicates the linearity of a detector based on the signal intensity, was determined to be 0.99710, indicating a good linear responsivity. The characterization results suggest that the radiation detectors based on SiPM- and CsI(Tl) can replace the currently used PMT-based radiation detector in an underwater environment.

Keywords: Detector design and construction technologies and materials; Dosimetry concepts and apparatus; Scintillators and scintillating fibres and light guides

[1] Corresponding author.

https://doi.org/10.1088/1748-0221/15/04/P04013

2020 JINST 15 P04013

Contents

2020 JINST 15 P04013

1 Introduction

A number of countries including the United States, Japan, China, and Russia are planning to build more nuclear power plants for electricity generation. In China, 45 nuclear power plants are in operation, about 15 are under construction, and more are about to be constructed. The ones under construction or at the planning stage are located mostly on the eastern coast of China [1]. Being located on the coast, these could have an adverse impact on marine life in case of a nuclear accident, and it can damage the world by ocean current. This can be learned from the case of the accident at Fukushima Daiichi nuclear power plant [2]. Therefore, it is necessary to develop a system for the early detection of radiation leak and nuclear power plants accident.

Sampling method and in-situ method are used to detect radioactive contamination in an underwater environment. Although sampling method is used to measure the level of radioactive contamination, and it can provide quantitative and qualitative results, it requires a long period of time to sampling and pretreat the samples and analyze the radioactivity in the samples. Sampling analysis also lacks the capability of immediate monitoring [3]. In-situ method enables real-time measurement of radioactivity in an underwater environment. The photomultiplier tube (PMT) has often been used as a light sensor for radiation detectors of in-situ type. However, the PMT has disadvantages like low photon detection efficiency, high cost, and high power consumption as compared with a silicon photomultiplier (SiPM) [4]. To replace the PMT and overcome these problems, we developed a radiation detector using an SiPM, which has low cost, and low power consumption with a CsI(Tl) scintillator.

2 Materials and methods

Figure 1 shows a schematic of the underwater radiation monitoring system using an SiPM. The system comprises of a detecting element for converting the incoming radiation into electrical signals, a signal processing element for amplifying and shaping the electrical signals, and a display element for displaying the data. The detecting element consists of a CsI(Tl) scintillator, SiPM, and light guide (figure 2). In general, NaI(Tl) scintillators are used as the radiation detecting component. However, due to the high-humidity in an underwater environment, a NaI(Tl) scintillator is not

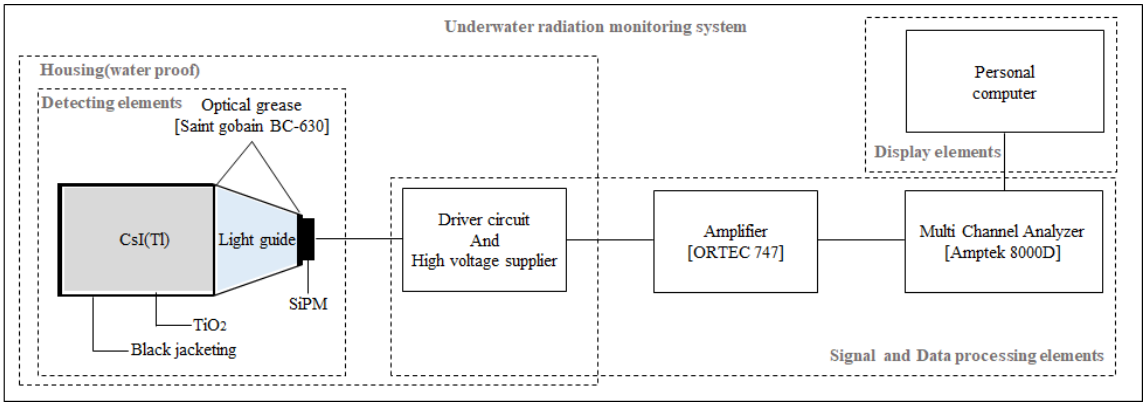

Figure 1. Schematic of the underwater radiation monitoring system.

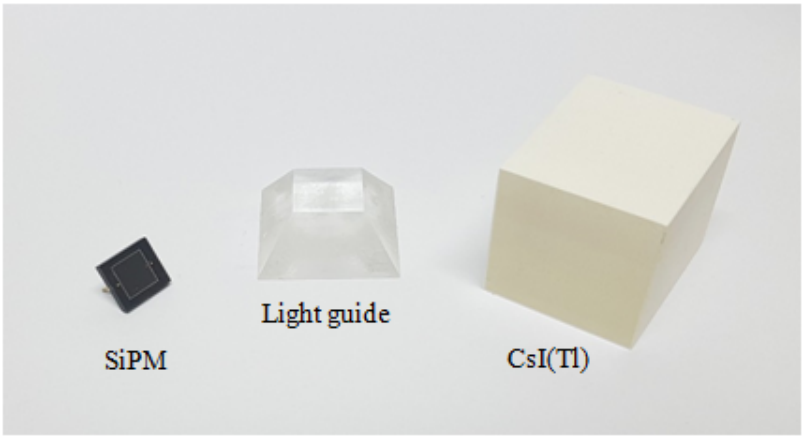

Figure 2. Components of the detecting element.

suitable because of its high hygroscopicity. In this study, CsI(Tl) scintillator is used instead of NaI(Tl), due to properties such as high density, high light emission efficiency of 52,000 photons per 1 MeV of the incoming gamma ray, similar refractive index to glass, and low hygroscopicity [5–7]. The size of CsI(Tl) scintillator is 25.4 mm × 25.4 mm, and the thickness was fixed at 30 mm to sufficiently absorb the emission energy of ^{137}Cs. Further, to decrease the loss of internally emitted photons before reaching the SiPM, a 0.33 mm thick TiO_2 reflector was deposited. Table 1 lists the specifications of the CsI(Tl) and NaI(Tl) scintillators.

Table 1. Specifications of the CsI(Tl) and NaI(Tl) scintillators.

Property	CsI(Tl)	NaI(Tl)
Density (g/cm^3)	4.15	3.67
Light output (photon/MeV)	52,000	38,000
Decay time (ns)	1000	250
Emission wavelength (nm)	550	415
Refractive index	1.80	1.85
Hygroscopic	Slightly	Yes

2020 JINST 15 P04013

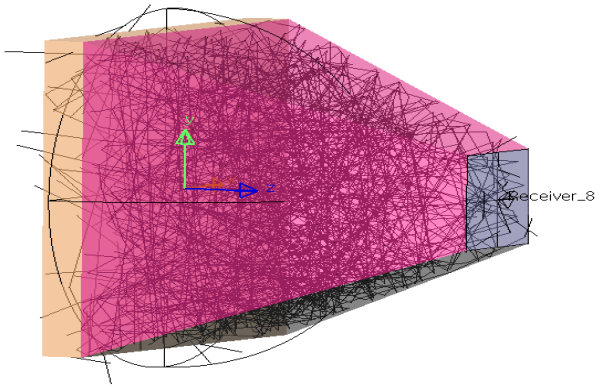

Figure 3. Geometry of the light guide obtained using optical simulation.

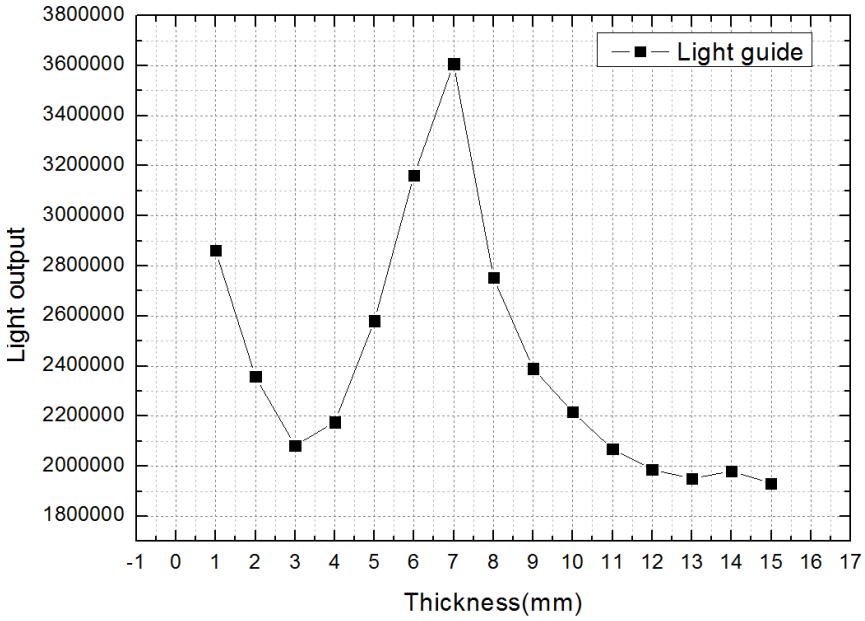

Figure 4. Result of the optical simulation.

SiPMs (S13360-6050PE model, manufactured by Hamamatsu Photonics) with areas of 6 mm × 6 mm each were used in this study. A polymethylmethacrylate (PMMA)-based light guide (manufactured by Epic Crystal) was used to reduce the photon loss because of the difference between the SiPM area and CsI(Tl) scintillator area. Because specifications such as the thickness of the material and internal reflection angle affect the photon transfer efficiency when using a light guide, an optical simulation program was used to simulate and optimize the thickness of the light wave [8]. Figure 3 presents the geometry of the light guide obtained using optical simulation and figure 4 illustrates the result of the simulation. The input wavelength was chosen as 520 nm, which is the emission wavelength of the CsI(Tl) scintillator, and the surface of the light guide was coated with a material having 95% reflectance. The thickness of the optimized light guide is 7 mm.

To minimize the light loss occurring when bonding, we used optical grease (BC-630 model, manufactured by Saint-Gobain), which has a refractive index of 1.465 and optical transmittance

2020 JINST 15 P04013

of 95% in the spectral range of 280–700 nm [10]. The light guide surface was wrapped with Teflon tape. Then, the external surface was wrapped with a dark tape to remove any noise due to external light.

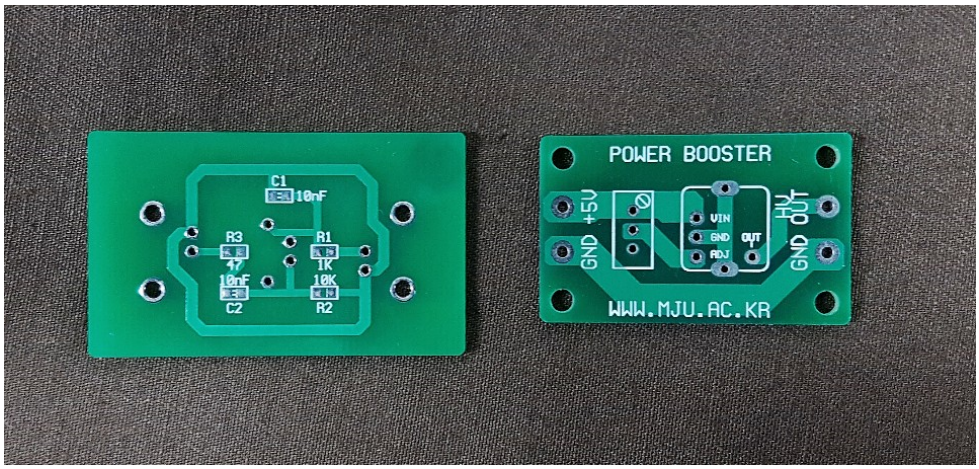

Figure 5. Driver circuit (left) and high voltage supply circuit (right).

Figure 5 shows the driver and high voltage supply circuits. The recommend voltage of SiPM is threshold voltage plus 3 V. The threshold voltage of SiPM used in this study is 53.5 V, so the applied voltage is 56.5 V. The high voltage supply circuit was designed using UltraVolt power supply (manufactured by Advanced Energy) that can supply voltages from 0 V to 100 V with a ripple noise below 50 mV.

Signals from SiPM are delivered to an amplifier (575A, ORTEC) for amplification and molding. The 575A amplifier can amplify signals from 2 times up to 100 times. The molding time can be set to 0.5, 1.5, or 3 µs. The amplified and molded signals are transferred to a multichannel analyzer (MCA-8000D, Amptek), which has characteristics such as high velocity ADC (100 MHz, 16 bit), 8000 channels, and a conversion time of 10 ns. The signals are displayed through a PC program.

Figure 6 presents a diagram of the detector housing and its photo. The housing should ensure that the underwater radiation detector is waterproof. The detector cover is designed with acetal, which is the optimum enclosure material for intermediate water masses (up to 400 m) since it exhibits low linear attenuation coefficient values [10]. The detector bracket enables us to adjust the scintillator size from 3 cm to 5 cm. The housing is tested for waterproofing based on the IEC 60529 standard and it satisfies the conditions of IP68. We used a 1 m waterproof cable.

The fabricated underwater radiation detector was tested using standard radiation sources and a liquid radiation source. The standard sources include ^{137}Cs (662 keV) with a half-life of 30.17 years, ^{70}Co (122 keV) with a half-life of 271 days, ^{133}Ba (356 keV) with a half-life of 10.51 years, and ^{60}Co (1173 keV and 1332 keV) with a half-life of 5.27 years. The values within brackets denote the respective energy peaks. The liquid radiation source (^{137}Cs) has a radioactivity of 9.91 ±0.18 Bq/g. To produce radioactive contaminated water which can be generated in an accident or radiation leakage, the liquid radiation source was diluted with distilled water. The radioactivity of contaminated water ranges from 38.71 Bq/L to 4955 Bq/L.

2020 JINST 15 P04013

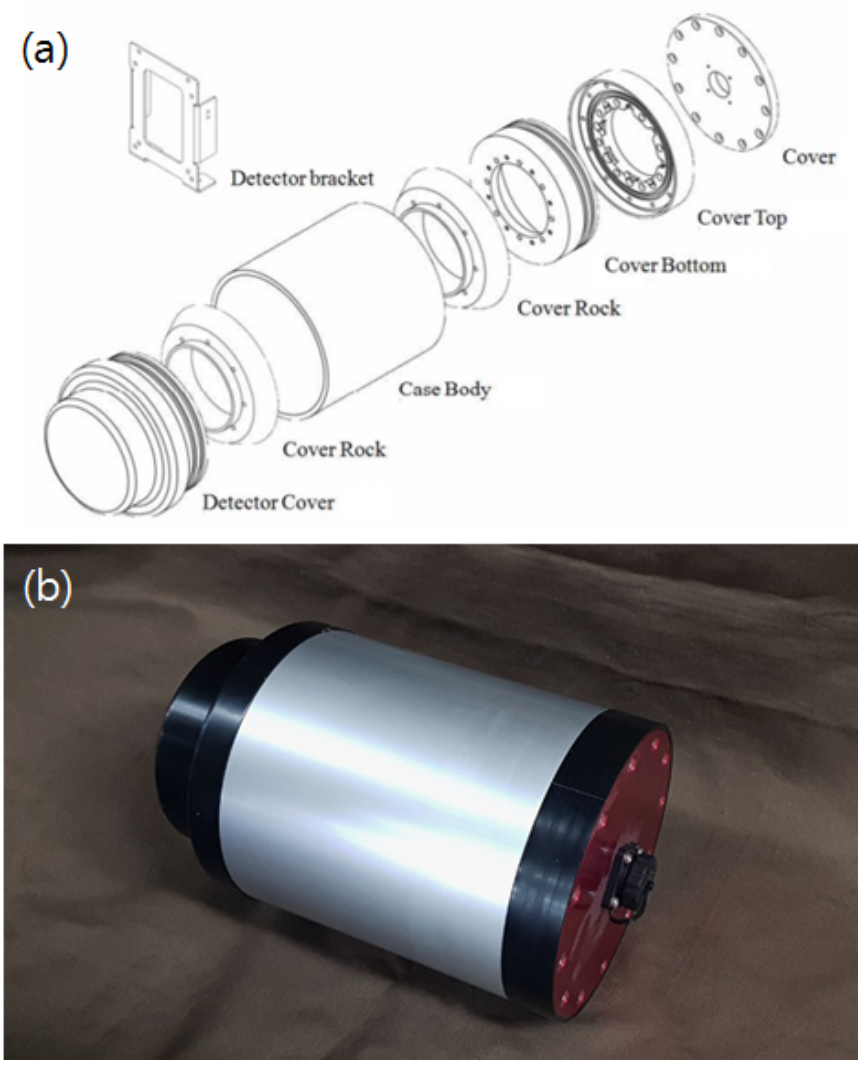

Figure 6. (a) Diagram of detector housing, and (b) photo of the housing.

3 Results and discussion

Energy resolution is the most important factor when measuring the energy of incident radiation. The absolute energy resolution is usually defined as the full width at half maximum (FWHM) to be measured, and it is considered impossible to decompose when energy less than this value is in close proximity. Figure 7 shows the energy spectra using the underwater radiation detector. The 122 keV peak of the ^{57}Co source exhibits an energy resolution of 18.12 ± 0.20%. The 356 keV peak in the ^{133}Ba spectrum yields an energy resolution of 10.91 ± 0.10%. The 662 keV peak of ^{137}Cs exhibits an energy resolution of 8.84 ± 0.08%, whereas an energy resolution of 4.55 ± 0.02% is obtained for the 1332 keV peak of ^{60}Co.

Figure 8 shows the energy spectra of a mixed radiation source. We observe that the peaks of the different sources are clearly distinguishable. Figure 9 shows the energy calibration line of the underwater radiation detector using the data from figure 8. When radiation enters the scintillator,

2020 JINST 15 P04013

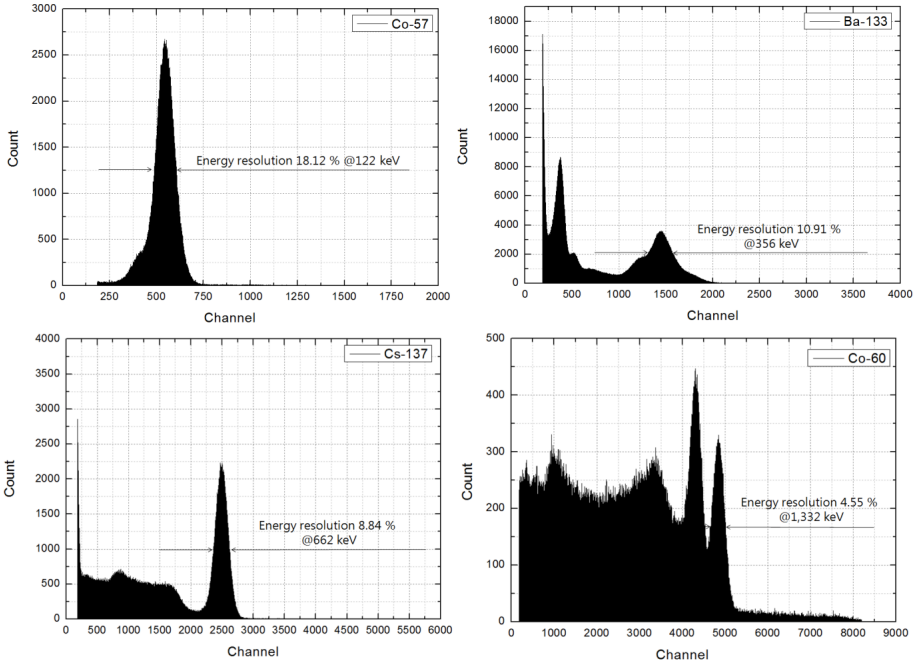

Figure 7. Measured energy spectra for ^{57}Co (122 keV), ^{133}Ba (356 keV), ^{137}Cs (662 keV), and ^{60}Co (1173 and 1332 keV).

it will emit photons depending on the gamma ray energy. Photons are converted to a pulse by a photosensor, and the magnitude of the pulse is proportional to the number of photons emitted from the scintillator. This pulse is classified into the channels according to the size. Therefore, the linearity of energy is an important factor for analyzing the nuclide. The points on this graph were obtained from figure 9, and the line was estimated based on the measured photopeak energies and channel numbers of radiation source. The fit, shown in figure 9, confirms the linearity of the relationship between the gamma-ray energy and peak channel number for energies ranging from 122 to 1332 keV. R-squared is the root mean square value and is commonly used for analyzing the difference between a theoretical value and the measured value [9]. The R-squared value corresponding to this linear fit is found to be 0.99937.

$$\overline{X} = \sum \frac{X_i}{n}$$

$$\sigma(X) = \sqrt{\frac{\left(X_i - \overline{X}\right)^2}{n-1}}$$

$$\sigma\left(\overline{X}\right) = \frac{\sigma(X)}{\sqrt{n}}$$

Table 2 lists 10 measurements at the background and 38.71 Bq/L. The equation below the table is an equation for calculating the standard uncertainty where $\overline{X}$ denotes the average of the measurements, σ(X) denotes the standard deviation of the measurements, and $\sigma\left(\overline{X}\right)$ denotes the standard deviation of the averages. Figure 10 shows the energy spectra of the underwater radiation detector. Measurements were performed for the activity due to ^{137}Cs (38.71–4955 Bq/L) as well

2020 JINST 15 P04013

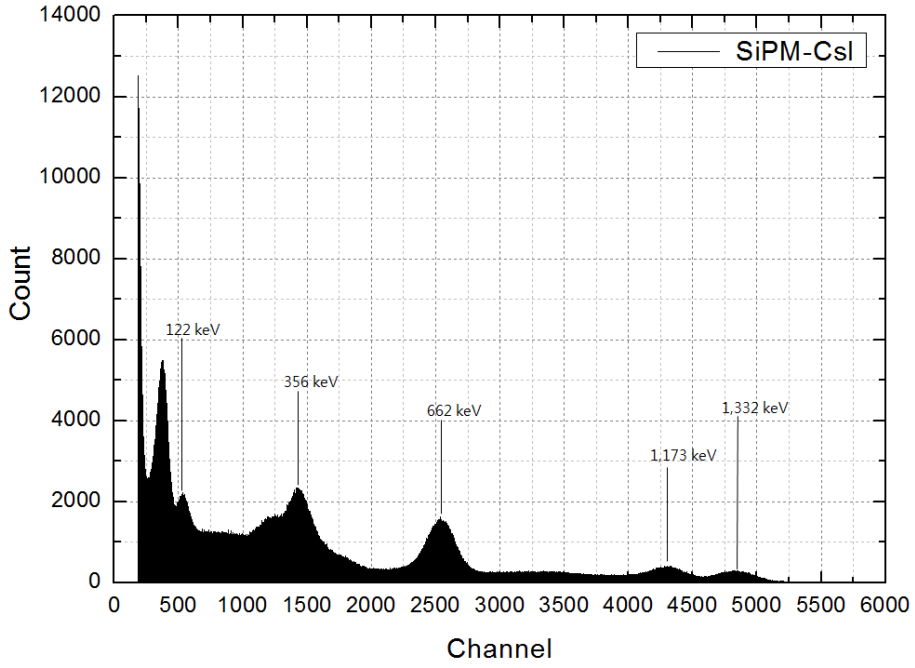

Figure 8. Energy spectra of mixed gamma-rays emitted from ^{57}Co (122 keV), ^{133}Ba(356 keV), ^{137}Cs (662 keV), and ^{60}Co (1173 and 1332 keV).

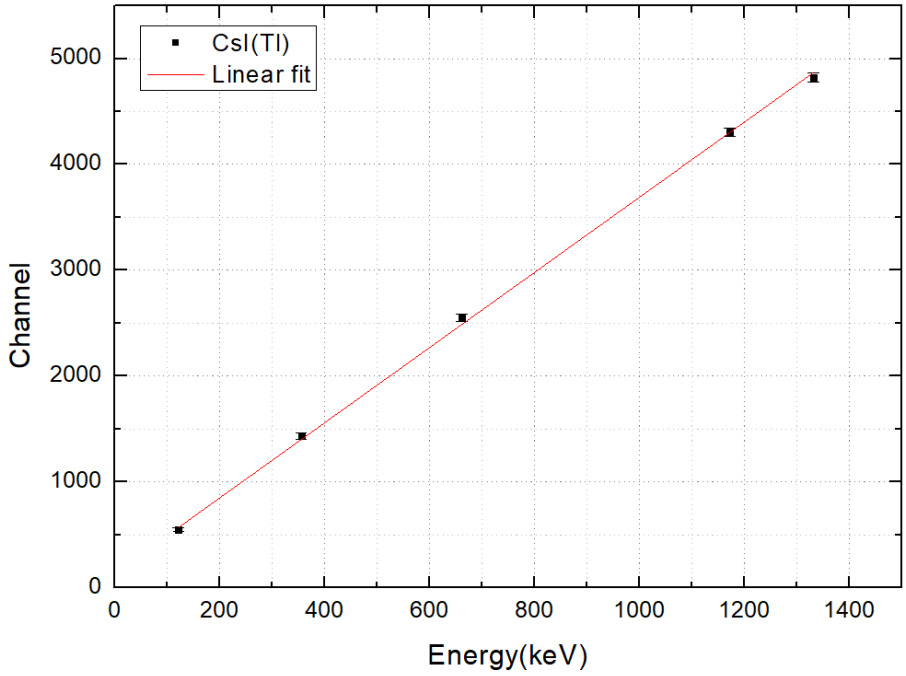

Figure 9. Linear fit of the measured photopeak energies of ^{57}Co (122 keV), ^{133}Ba (356 keV), ^{137}Cs (662 keV), and ^{60}Co (1173 and 1332 keV) and channel number.

2020 JINST 15 P04013

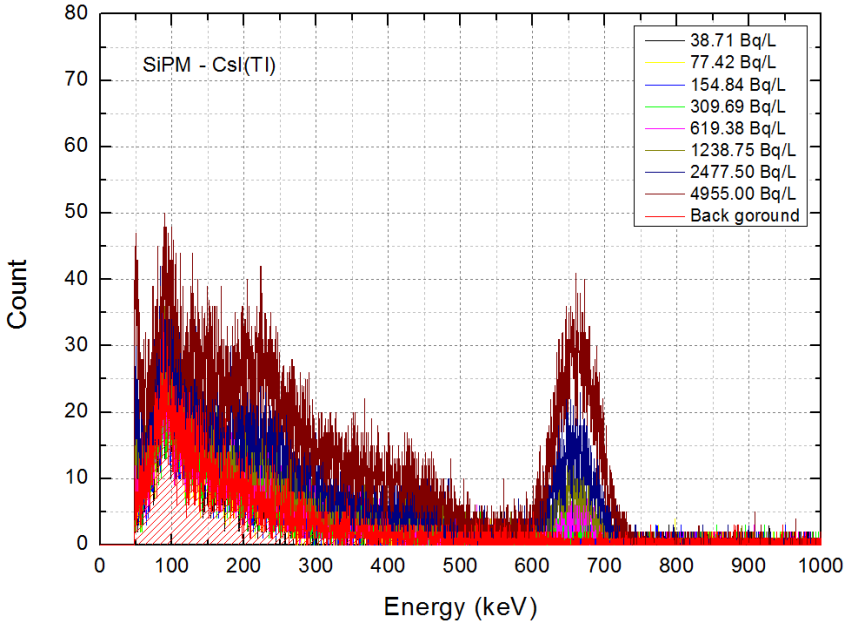

Figure 10. Energy spectra of the underwater radiation detector with radioactivity of the liquid sample (^{137}Cs).

Table 2. 10 measurements using Underwater radiation detector at background and 38.71 Bq/L.

Number	Background	38.71 Bq/L
1	0.61	0.74
2	0.61	0.74
3	0.60	0.73
4	0.60	0.75
5	0.62	0.74
6	0.61	0.73
7	0.61	0.76
8	0.62	0.72
9	0.61	0.74
10	0.60	0.74
Average	**0.61**	**0.74**

as the background radiation. The average background count from 10 measurements is 0.61 cps (counts per second), and the uncertainty is 0.0046 (95% C.L). The average count corresponding to 38.71 Bq/L is 0.74 cps, and the uncertainty is 0.0070 (95% C.L). The difference between the background and minimum concentration is 0.13 cps. The incremental ratio, obtained using the following equation, is 21.31%, where N is the count rate at 38.71 Bq/L and N_{BKG} is the background count rate [11].

$$\text{Incremetal ratio } (\%) = \frac{N - N_{\mathrm{BKG}}}{N_{\mathrm{BKG}}} \times 100\%$$

Figure 11 shows the linearity of the underwater radiation detector using the net count rate ($\mathrm{N_{MEASUREMENT}} - \mathrm{N_{BKG}}$) from 38.71–4955 Bq/L for the ^{137}Cs sample. With the decrease in

2020 JINST 15 P04013

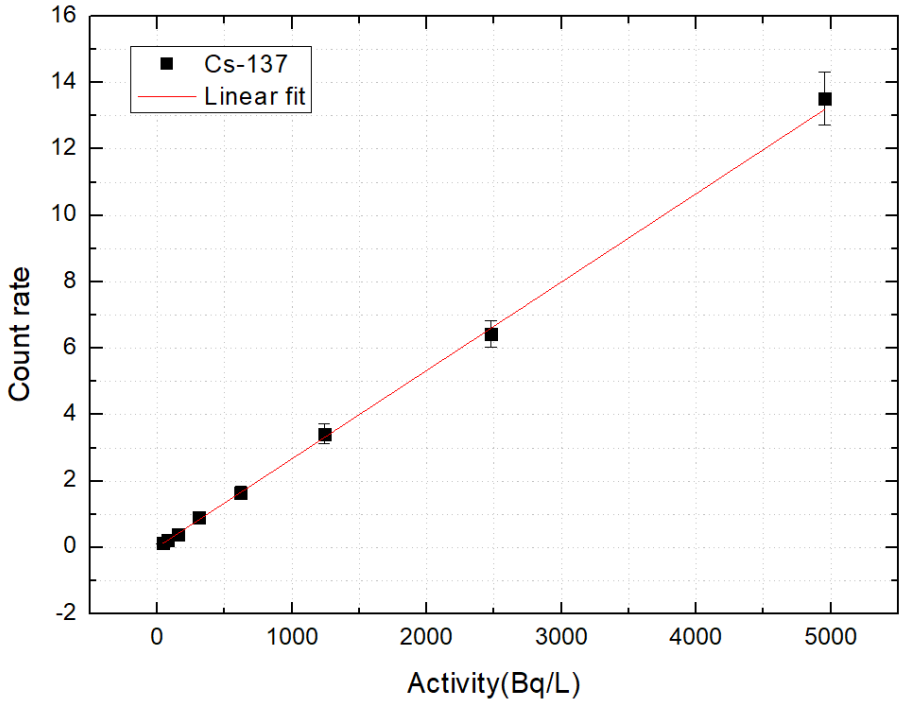

Figure 11. Linearity of the underwater radiation detector in terms of radioactivity of the liquid sample (^{137}Cs).

intensity of the radioactive sources, the radiation flux per unit area decreases linearly and so does the detection capability of the detector. This is a very important factor in evaluating the reliability of a detector. The results show an R-squared value of 0.99710, confirming a good linearity characteristic.

4 Conclusions

In this paper, the development of an underwater radiation detector using SiPM, CsI(Tl) and a light guide was presented. The SiPM was chosen instead of the currently used PMT owing to its superior characteristics such as high photon detection efficiency, low applied voltage (power consumption), and high gain. The CsI(Tl) inorganic scintillator was used instead of NaI(Tl) because it possesses better responsivity for gamma rays (owing to its high density) and better photon emittance per incident unit energy. Further, to minimize the light loss due to area mismatch between the SiPM and CsI(Tl) scintillator, a light guide was designed using an optical simulation program. The characteristics of the fabricated radiation detector were evaluated using standard radiation sources (^{57}Co, ^{133}Ba, ^{137}Cs, and ^{60}Co) and a liquid source (^{137}Cs, 38.71–4955 Bq/L). The characterization results confirmed that all the characteristics including energy resolution, energy linearity, and response linearity according to the concentration of the radioactive contaminated water were excellent. Moreover, a 38.71 Bq/L source can be detected with a 3 sigma significance in at least 4 hours. In view of these results, the SiPM-based detector can be used in an underwater environment instead of the existing PMT in commercial products.

2020 JINST 15 P04013

Acknowledgments

This work was supported by the Korea Institute of Energy Technology Evaluation and Planning (KETEP) and the Ministry of Trade, Industry and Energy (MOTIE) of the Republic of Korea (Grant No. 20171520101720).

References

[1] *Nuclear Power in China*, (2018), http://www.world-nuclear.org/information-library/country-profiles/countries-a-f/china-nuclear-power.aspx(Accessed January 8, 2019).

[2] J. Kanda, *Continuing ^{137}Cs release to the sea from the Fukushima Dai-ichi nuclear power plant through 2012*, *Biogeosciences* **10** (2013) 6107.

[3] J.H. Kim, K.H. Park and K.S. Joo, *Development of low-cost, compact, real-time, and wireless radiation monitoring system in underwater environment*, *Nucl. Eng. Technol.* **50** (2018) 801.

[4] B. Sanaei, M.T. Baei and S.Z. Sayyed-Alangi, *Characterization of a new silicon photomultiplier in comparison with a conventional photomultiplier tube*, *J. Mod. Phys.* **6** (2015) 425.

[5] H.M. Park and K.S. Joo, *Remote radiation sensing module based on a silicon photomultiplier for industrial applications*, *Appl. Radiat. Isot.* **115** (2016) 13.

[6] H. Yoo, S. Joo, S. Yang and G. Cho, *Optimal design of a CsI (Tl) crystal in a SiPM based compact radiation sensor*, *Radiat. Meas.* **82** (2015) 102.

[7] M. Grodzicka, M. Moszyński, T. Szczęśniak, M. Kapusta, M. Szawłowski and D. Wolski, *Energy resolution of small scintillation detectors with SiPM light readout*, 2013 *JINST* **8** P02017.

[8] H.M. Park et al., *Evaluation of the photon transmission efficiency of light guides used in scintillation detectors using LightTools code*, *J. Radiat. Prot. Res.* **41** (2016) 282.

[9] J. Kim, K. Park and K. Joo, *Feasibility of miniature radiation portal monitor for measurement of radioactivity contamination in flowing water in pipe*, 2018 *JINST* **13** P01022.

[10] J.G. Park, S.H. Jung, J. Moon, D. Oh, S. Kang and Y. Kim, *Determination of effective detection distance and minimum detectable activity for radiation monitoring system in water*, *J, Radiat. Ind.* **12** (2018) 11.

[11] C. Tsabaris. G. Androulakaki, S. Alexakis and D.L. Patiris, *An in-situ gamma-ray spectrometer for the deep ocean*, *Appl. Radiat. Isot.* **142** (2018) 120.

2020 JINST 15 P04013